Chapter 2
Beam Dynamics

E. Wilson and B. J. Holzer

2.1 Linear Transverse Beam Dynamics

Now let us look in detail at the motion of particles in the transverse coordinates of the coordinate system defined in Fig. 2.1.

2.1.1 Co-ordinate System

The guide field of a synchrotron is usually vertically directed, causing the particle to follow a curved path in the horizontal plane (Fig. 2.1). The force guiding the particle in a circle is horizontal and is given by:

$$\boldsymbol{F} = e \cdot \boldsymbol{v} \times \boldsymbol{B}, \tag{2.1}$$

where:

$\boldsymbol{v}$ is the velocity of the charged particle in the direction tangential to its path,
$\boldsymbol{B}$ is the magnetic guide field.

The guide field inside a dipole magnet is uniform and the ideal motion of the particle is simply a circle of (local) radius of curvature, $\rho(s)$. The trajectory of an ideal particle (ideal in energy and without any amplitude) that is defined by the arrangement of the dipole magnets is called *design orbit*. The machine is usually designed with this orbit at the centre of its vacuum chamber. Now there is no such

E. Wilson · B. J. Holzer (✉)
CERN (European Organization for Nuclear Research), Meyrin, Geneva, Switzerland
e-mail: Bernhard.holzer@cern.ch

S. Myers, H. Schopper (eds.), *Particle Physics Reference Library*,
https://doi.org/10.1007/978-3-030-34245-6_2

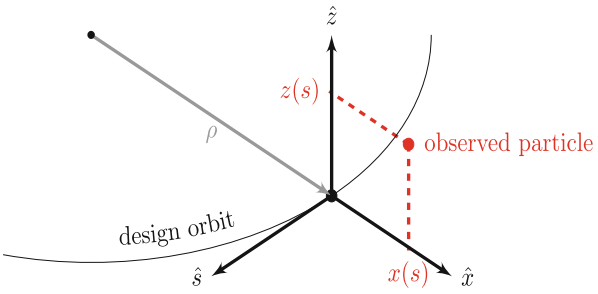

Fig. 2.1 Charged particle orbit in magnetic field

thing as an ideal particle. Still, we shall suppose that it is possible to find an orbit or curved path for the non-ideal particle which closes on itself around the synchrotron, which we call the *closed* or *equilibrium orbit* and it should be close enough to the ideal design orbit.

2.1.2 Displacement and Divergence

A beam of particles enters the machine as a bundle of trajectories spread about the ideal orbit. At any instant a particle may be displaced horizontally by x and vertically by z from the ideal position and may also have divergence angles horizontally and vertically:

$$x' = dx/ds, \quad \text{and } z' = dz/ds. \tag{2.2}$$

The divergence would cause particles to leave the vacuum pipe except for the carefully shaped field which restores them back towards the beam centre so that they oscillate about the ideal orbit. The design of the restoring fields determines the transverse excursions of the beam and the size of the cross section of the magnets and is therefore of crucial importance to the cost of a project.

2.1.3 Bending Magnets and Magnetic Rigidity

The design of a synchrotron; the diameter of the ring and its sheer size and cost for a given energy is driven by the fact that bending particle trajectories depends on a magnetic rigidity. The rigidity increases with momentum and is a function of the bending field which, for room temperature magnets, saturates at about 2 T.

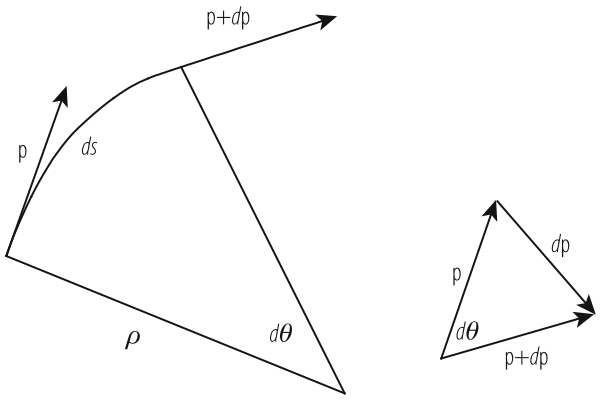

Fig. 2.2 Vector diagram showing differential changes in momentum for a particle trajectory

We will now briefly derive an expression for the magnetic rigidity of a relativistic. A particle has a relativistic momentum vector $\boldsymbol{p}$ and travels perpendicular to a field $\boldsymbol{B}$ which is into the plane of the diagram (Fig. 2.2).

We write the Lorentz force on the particle on its circular path as

$$\boldsymbol{F}_{Lorentz} = e * (\boldsymbol{v} \times \boldsymbol{B})$$

Assuming an idealized homogeneous dipole magnet along the particle orbit, having pure vertical field lines, the condition for a perfect circular orbit is defined as equality between this Lorentz force and the centrifugal force.

$$\boldsymbol{F}_{centrifugal} = \frac{\gamma m v^2}{\rho}$$

This yields the following condition for the idealized ring:

$$B\rho = \frac{p}{e}$$

where we are referring to protons and have accordingly set q = e. We conclude that the beam rigidity Bρ, given by the magnetic field and the size of the machine, defines the momentum of a particle that can be carried in the storage ring, or in other words, it ultimately defines, for a given particle energy, the magnetic field of the dipole magnets and the size of the storage ring.

We really should use the units Newton-second for p and express e in Coulombs to give $(B\rho)$ in Tesla·metres. However, in charged particle dynamics we often talk in a careless way about the 'momentum' pc. This actually has the dimensions of an energy and is expressed in units of GeV.

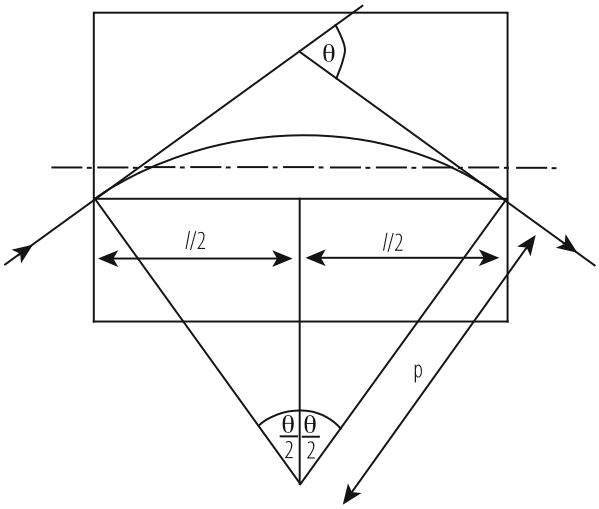

Fig. 2.3 Geometry of a particle trajectory in a bending magnet of length ℓ and deflecting angle θ

A useful rule of thumb formula based on these units is:

$$B\rho \ [\mathrm{T} \cdot \mathrm{m}\ ] = 3.3356 \ pc \ [\mathrm{GeV}\ ]\,. \tag{2.3}$$

2.1.4 Particle Trajectory in a Dipole Bending Magnet

The trajectory of a particle in a bending magnet or dipole of length ℓ is shown in Fig. 2.3. Usually the magnet is placed symmetrically about the arc of the particle's path. One may see from the geometry that:

$$\sin(\theta/2) = \frac{\ell}{2\varrho} = \frac{\ell B}{2\,(B\varrho)}, \tag{2.4}$$

and, if $\theta << \pi/2$

$$\theta \approx \frac{\ell B}{(B\varrho)}. \tag{2.5}$$

So the bending angle provided by a dipole magnet is given by the ration of its integrated field strength and the beam rigidity.

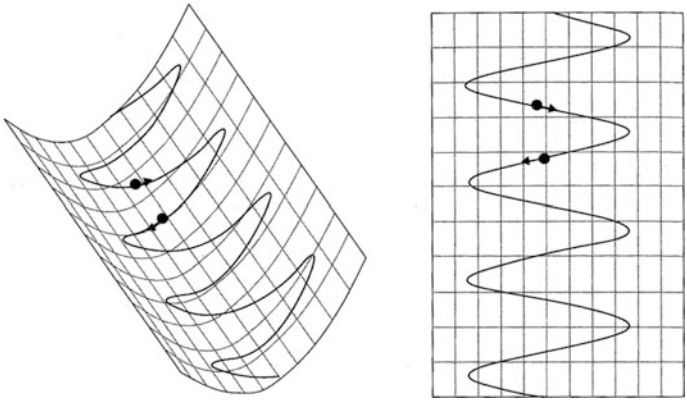

Fig. 2.4 Two views of a sphere rolling down a gutter as it is focused by the walls

2.1.5 Weak Focusing

We have mentioned that cyclotrons and early synchrotrons relied on weak focusing to constrain circulating particles within the vacuum chamber. In order to provide this, the vertical guide field has a slight negative gradient in the radial direction around the rim of the accelerator. The field lines belly out from the outer gap of the magnet. It can be shown, by applying $\nabla \times \overline{\boldsymbol{B}} = \mathbf{0}$, that there will be horizontal field components in this region. These produce vertically directed forces on errant particles causing them to oscillate about the median plane in a potential well (Fig. 2.4).

The motion is analogous to a small sphere rolling down a slightly inclined gutter with constant speed. Figure 2.4 shows two views of this motion and from the bottom view we recognise the motion as a sine wave. Note too that the sphere makes four complete oscillations along the gutter. In the language of accelerators, its motion has a wave number or "tune", $Q = 4$.

To complete the analogy of a weak focusing synchrotron we imagine that we bend the gutter into a circle rather like the brim of a hat. We provide the necessary instrumentation to measure the displacement of the sphere from the centre of the gutter each time it passes a given mark on the brim and we also have a means to measure its transverse velocity. With the aid of a computer, we might convert this information into the divergence angle, which is used as vertical axis in Fig. 2.5:

$$x' = \frac{dx}{ds} = \frac{v_\perp}{v_\parallel}. \tag{2.6}$$

We can make a ring shaped gutter out of a slightly different length of gutter than is shown so that Q is not an integer. We can plot a point for each arrival of

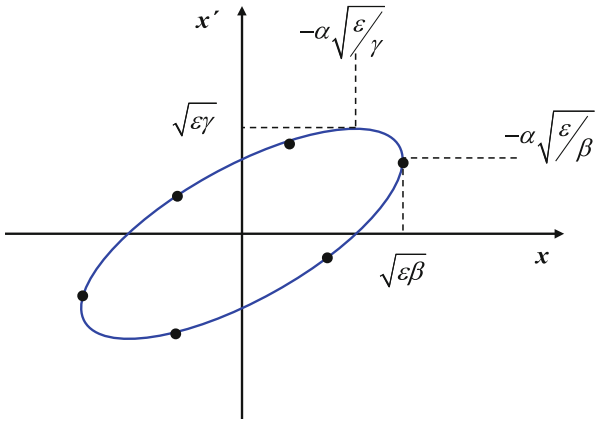

Fig. 2.5 The elliptical locus of a particle's history in phase space as it circulates in a synchrotron

the sphere in a diagram of x' against x which we call a 'phase space diagram' of transverse motion. The sphere has a large transverse velocity as it crosses the axis of the gutter and has almost zero transverse velocity as it reaches its maximum displacement.

If we plot these 'observations' they will be an ellipse (Fig. 2.5) and the phase of the oscillator will advance by Q evolutions each time the particle returns. Of course, only the fractional part of Q may be deduced from our observations since our measurements do not reveal what happens round the rest of the hat's brim.

Now let us use the analogy to define some of the transverse dynamical quantities of a particle beam. The area of the ellipse is a measure of how much the particle departs from the ideal trajectory, represented in the diagram by the origin.

$$\text{Area} = \pi\varepsilon \ \ [\text{mm} \cdot \text{rad}]\,. \tag{2.7}$$

In accelerator notation we use ε, the product of the semi-axes of the ellipse as a measure of the area called the emittance. The emittance is usually quoted in units of π mm·mradians. Thus if the semi-axes are 1 mm and 1 mrad the emittance will be 1 mm·mradian but the area will be π mm·mradian. The maximum excursion in displacement, the major axis, of the ellipse is defined as:

$$\hat{x} = \sqrt{\varepsilon\beta}, \tag{2.8}$$

At locations where the beta function reaches an extremum, i.e. $\alpha = 0$, we obtain hence

$$\hat{x}' = \sqrt{\varepsilon/\beta}. \tag{2.9}$$

We shall see that β (later to be called the envelope or betatron function) is a property of the gutter, not the beam. In the synchrotron it varies around the ring and is the envelope function we have plotted in Fig. 2.10 and again in Fig. 2.11. By analogy, the "brim of the hat" which represents the alternating gradient focusing system shown in this figure will vary its width and curvature around the crown and β will follow this variation in some way.

2.1.6 *Alternating Gradient Focusing*

In Chap. 1 we described a major break-through in the design of synchrotrons: the discovery of alternating gradient (AG) focusing (see [1] for an excellent summary of the dynamics of AG focussing). This allowed designers to use much stronger focusing systems with considerable savings in the space needed for the beam cross section.

The principle is shown in Fig. 2.6 which depicts an optical system in which each lens is concave in one plane while convex in the other and they alternate. It is possible, even with lenses of equal strength, to find a ray which is always on axis at the D lenses in the horizontal plane and therefore only sees the F lenses. To appear like Fig. 2.6 the spacing of the lenses would have to be $2f$. If the ray is also central in the lenses which are vertically defocusing, the same condition will apply simultaneously in the vertical plane. At least one particular particle or trajectory corresponding to this ray will never be defocused and be contained indefinitely.

The alternating gradient idea will work even when the rays in the D lenses do not pass exactly at their centre and the lenses are not spaced by precisely $2f$. In fact it is sufficient for the lens strengths and spacing to be chosen to ensure that the particle trajectories *tend* to be closer to the axis in D lenses than in F lenses as shown in Fig. 2.10.

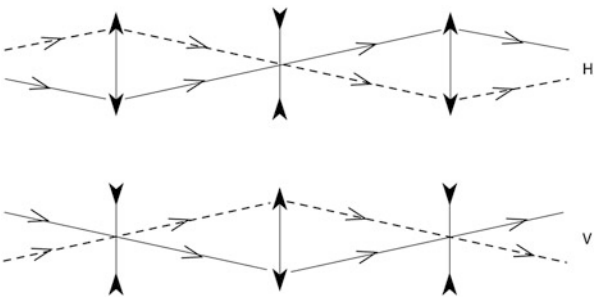

Fig. 2.6 Optical analogy with an alternating pattern of lenses

2.1.7 *Quadrupole Magnets*

The first alternating gradient synchrotorns used alternating magnetic lenses formed by bending magnets having the same vertical guide field but a radial gradient of alternating sign. In a modern synchrotron the functions of guiding and focussing the beam are separated. The dipole magnets which do the guiding have no gradient. The principal focusing elements are quite a different kind of magnet with four poles which produce gradient but no bending. The poles of these quadrupole magnets are truncated rectangular hyperbolae and alternate in polarity around the aperture circle which just touches the poles.

Figure 2.7 shows a particle's view of the fields and forces in the aperture of a quadrupole as it passes through normal to the plane of the paper. The field shape is such that it is zero on the axis of the device but its strength rises linearly with distance from the axis. This can be seen from a superficial examination of Fig. 2.7 if we remember that the product of field and length of any field line joining the poles is a constant. Symmetry tells us that the field is vertical in the median plane (and purely horizontal in the vertical plane of asymmetry). The field must be downwards on the left of the axis if it is upwards on the right.

The horizontal focusing force, $-evB_z$, has an inward direction on both sides and, like the restoring force on a weight suspended from a spring, rises linearly with displacement, x. The strength of the quadrupole is characterised by its gradient dB_z/dx normalised with respect to magnetic rigidity:

$$k = \frac{1}{(B\varrho)} \frac{dB_z}{dx}. \tag{2.10}$$

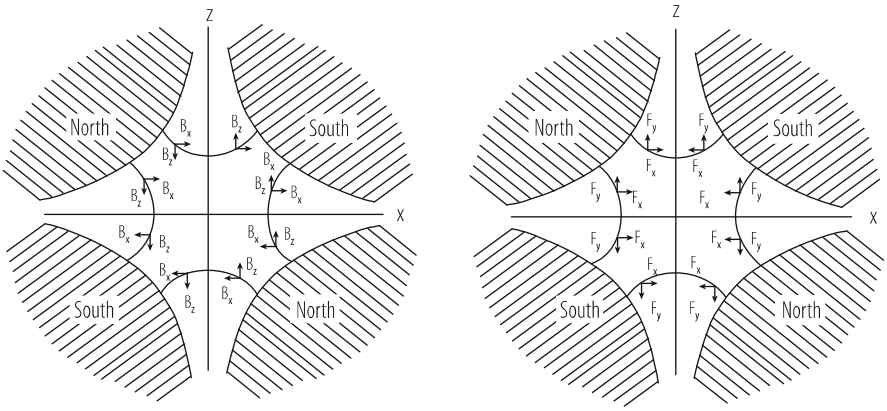

Fig. 2.7 Components of field and force in a magnetic quadrupole. Positive ions approach the reader on paths parallel to the s axis (orthogonal to x and z) [2]

The angular deflection given to a particle passing through a short quadrupole of length, ℓ and strength k, at a displacement x is therefore:

$$\Delta x' = \theta = \ell B/(B\rho) = \ell B' x/(B\rho) = \ell k x. \tag{2.11}$$

The use of x' to indicate the divergence angle of a trajectory is defined in Fig. 2.5. Compare this with a converging lens in optics:

$$\Delta x' = -x/f \tag{2.12}$$

and we see that the focal length of a horizontally focusing quadrupole is

$$f = -1/(k\ell) \tag{2.13}$$

The particular quadrupole shown in Fig. 2.7 would focus positive particles coming out of the paper or negative particles going into the paper in the horizontal plane. A closer examination reveals that such a quadrupole deflects particles with a vertical displacement away from the axis—vertical displacements are defocused. This can be seen if Fig. 2.7 is rotated through 90°.

2.1.8 The Equation of Motion

Earlier we derived an expression for the change in divergence of a particle passing through the quadrupole. A horizontally focusing quadrupole (which is at the same time vertically defocusing) has a negative k.

We first look at the vertical plane. The angular deflection given to a particle passing through a short quadrupole of length ds and strength k at a displacement z is therefore:

$$dz' = -kzds. \tag{2.14}$$

From this we can deduce a differential equation for the motion

$$z'' + k(s)z = 0. \tag{2.15}$$

Here we would like to make a clear statement: While inside a lattice element, say a quadrupole lens, the normalised gradient k is constant and we get a equation that we know from Hook's law in classical mechanics, (see Eq. 2.12), the situation now is more general. We allow $k(s)$ to change, while our particles are running through the accelerator. The corresponding equation (2.15) is called Hill's Equation, a second order linear equation with a periodic coefficient, $k(s)$ which describes the distribution of focusing strength around the ring. The above form of Hill's equation

applies to the motion in the vertical plane while in the horizontal plane the effect of the dipole magnets has to be included:

$$x'' + \left[\frac{1}{\rho^2(s)} - k(s)\right] x = 0. \tag{2.16}$$

Here the sign in front of $k(s)$ is reversed so that the quadrupole focuses. The extra focusing term $1/\rho^2$ due to the curvature of the orbit can be significant in small rings. In the old constant gradient synchrotrons, this weak focusing term was the only form of horizontal focusing.

We see in Fig. 2.10, the pattern of one cell of a simple synchrotron lattice—a pattern which is repeated many times around the circumference as may be seen in Fig. 2.11 which shows—in addition to the focusing and defocusing lenses also the bending magnets—bending magnets. Within this pattern of dipole and quadrupole focusing and defocusing (F and D), particles make betatron oscillations within the envelopes described by β_x and β_z, or more precisely, the square roots of these quantities (here we use the variable y to represent either the horizontal or the vertical coordinate, x or z)

$$y = \sqrt{\varepsilon\beta(s)}\sin\left(\phi(s) + \phi_0\right). \tag{2.17}$$

If one tries to verify that this is the solution of Hills Equation an important and necessary condition emerges:

$$\phi' = 1/\beta \tag{2.18}$$

From which we see that $2\pi\beta$ is the local wavelength of the transverse oscillations.

2.1.9 Matrix Description

Usually in alternating gradient (AG) machines, the ring is a repetitive pattern of focusing fields that we call the "lattice". Each lattice element may be expressed by a matrix and whole sections of the ring which transport the beam from place to place may be represented as the product matrix of the single element matrices involved, which makes the description of particle trajectories very simple and very elegant at the same time. Any linear differential equation, like Hill's Equation, has solutions which can be traced from one point, s_1, to another, s_2, by a 2×2 matrix, the transport matrix:

$$\begin{pmatrix} y(s_2) \\ y'(s_2) \end{pmatrix} = \begin{pmatrix} a & b \\ c & d \end{pmatrix} \begin{pmatrix} y(s_1) \\ y'(s_1) \end{pmatrix} = M_{21} \begin{pmatrix} y(s_1) \\ y'(s_1) \end{pmatrix}. \tag{2.19}$$

The transport matrix M_{21} has a rather simple form for each focusing quadrupole that the particle encounters and for the drift length between quadrupoles and it is easy to compute the four elements numerically once we define the length and focusing strength. We can trace particles by simply forming the product of these elementary matrices. But there is also a general relation between the elements a, b, c, d and the amplitude and phase of transverse motion between any two points. Each term in M_{21} can be expressed as a function of $\beta(s)$ and $\phi(s)$. The functions of $\beta(s)$ and $\phi(s)$ may be calculated by comparing the numerical result of multiplying the individual matrices for quadrupoles and drift lengths with what we know must be the general form of each element.

As a first step, we derive the general form of a periodic transport matrix.

To simplify the notation we drop the explicit dependence of β and ϕ on s from the expressions—we will just have to remember that they vary with s. We also introduce a new quantity:

$$w = \sqrt{\beta}. \tag{2.20}$$

just to avoid too many terms in what follows.

In this new notation we can write the solution of the Hill Equation:

$$y = \varepsilon^{1/2} w \, \cos(\varphi + \phi_0) \, . \tag{2.21}$$

Taking the derivative and substituting $\varphi' = 1/\beta = 1/w^2$ we have:

$$y' = \varepsilon^{1/2} w' \cos(\varphi + \phi_0) - \frac{\varepsilon^{\frac{1}{2}}}{w} \sin(\varphi + \phi_0) \, . \tag{2.22}$$

Next we substitute these explicit expressions for y and y' in both sides of the matrix equation. We do this first with the initial condition $\varphi_0 = 0$, this is the so-called 'cosine' solution, and then we do it again for the 'sine' solution with $\varphi_0 = \pi/2$. This is exactly equivalent to tracing the paraxial and central rays through an optical lens. We write $\phi_2 - \phi_1 = \phi$ for each case. Each of the two solutions give us two equations for y and y' and thus we obtain four simultaneous equations which can be solved for a, b, c, d in terms of w, w', and φ. The result is the most general form of the transport matrix between the positions s_1 and s_2 :

$$M_{12} = \begin{pmatrix} \frac{w_2}{w_1}\cos\varphi - w_2 w_1' \sin\varphi & w_1 w_2 \sin\varphi \\ -\frac{1+w_1 w_1' w_2 w_2'}{w_1 w_2}\sin\varphi - \left(\frac{w_1'}{w_2'} - \frac{w_2}{w_1}\right)\cos\varphi & \frac{w_1}{w_2}\cos\varphi + w_1 w_2' \sin\varphi \end{pmatrix}. \tag{2.23}$$

This rather formidable looking expression simplifies a lot, if we refer to a full circle, in other words, if we restrict M to apply between two identical points in successive turns or cells of a periodic structure. Then $w_2 = w_1$, $w_2' = w_1'$,

and φ to become μ, the phase advance per cell. The matrix for one period is now:

$$M = \begin{pmatrix} \cos\mu - ww'\sin\mu & w^2\sin\mu \\ -\frac{1+w^2w'^2}{w^2}\sin\mu & \cos\mu + ww'\sin\mu \end{pmatrix}. \tag{2.24}$$

Next we invent some new functions of β:

$$\begin{aligned} \beta &= w^2, \\ \alpha &= -ww' = -\tfrac{\beta'}{2}, \\ \gamma &= \tfrac{1+(ww')^2}{w^2} = \tfrac{1+\alpha^2}{\beta}. \end{aligned} \tag{2.25}$$

These functions (which are not the same as the parameters used in special relativity!) are a complete and compact description of the dynamics. The matrix now becomes even simpler:

$$M = \begin{pmatrix} \cos\mu + \alpha\sin\mu & \beta\sin\mu \\ -\gamma\sin\mu & \cos\mu - \alpha\sin\mu \end{pmatrix} = \begin{pmatrix} a & b \\ c & d \end{pmatrix}. \tag{2.26}$$

This is the Twiss matrix. It is the basic matrix for periodic lattices and should be memorized.

We can imagine that if we can only find an independent way of computing the numerical values of the four elements we can solve and find:

$$\begin{aligned} &\cos\mu = (\mathrm{Tr}\,\mathbf{M})/2 = (a+d)/2, \\ &\beta = b/\sin\mu > 0, \\ &\alpha = (a-b)/(2\sin\mu), \\ &\gamma = -c/\sin\mu. \end{aligned} \tag{2.27}$$

These Twiss parameters, μ, β, α, and γ, are therefore rigorously determined by the overall effect of the focusing properties of the lattice elements. Still, they vary around the ring and apply to the point chosen in the period as a starting and finishing point. We shall see that each individual component, quadrupole, dipole, or drift space in the ring has its own matrix and this provides the independent method of calculation. We must first choose the starting point, the location, s, where we wish to know β and the other Twiss parameters. By starting there and multiplying the element matrices together for one turn we are able to find a, b, c, d numerically for that location. We can then apply the above four equations to find the Twiss matrix. If the machine has a natural symmetry in which there are a number of identical periods, it is sufficient to do the multiplication up to the corresponding point in the next period. The values of α, β, and γ would be the same if we went on for the whole ring. By choosing different starting points we can trace $\beta(s)$ and $\alpha(s)$. We now give the matrices for the three basic lattice elements.

2.1.10 Transport Matrices for Lattice Components

An empty space or drift length is the simplest of the lattice component matrices. Figure 2.8(a) shows the analogy between a particle trajectory and a diverging ray in optics. The angle of the ray and the divergence of the trajectory are related:

$$\theta = \tan^{-1}\left(x'\right). \tag{2.28}$$

The effect of a drift length in phase space is a simple horizontal translation from (x, x') to $(x+\ell x', x')$ and can therefore be written as a matrix:

$$\begin{pmatrix} x_2 \\ x_2' \end{pmatrix} = \begin{pmatrix} 1 & \ell \\ 0 & 1 \end{pmatrix} \begin{pmatrix} x_1 \\ x_1' \end{pmatrix}. \tag{2.29}$$

The next case is that of a thin quadrupole magnet of infinitely small length but finite integrated gradient:

$$\ell k = \frac{1}{(B\rho)} \frac{\partial B_z}{\partial x}. \tag{2.30}$$

The optical analogy of a thin quadrupole with a converging lens is illustrated in Fig. 2.8(b). A ray, diverging from the focal point arrives at the lens at a displacement, x, and is turned parallel by a deflection:

$$\theta \approx \frac{1}{f} x. \tag{2.31}$$

This deflection will be the same for any ray at displacement x irrespective of its divergence. This behaviour can be expressed by a simple matrix, the thin lens matrix:

$$\begin{pmatrix} x_2 \\ x_2' \end{pmatrix} = \begin{pmatrix} 1 & 0 \\ -1/f & 1 \end{pmatrix} \begin{pmatrix} x_1 \\ x_1' \end{pmatrix}. \tag{2.32}$$

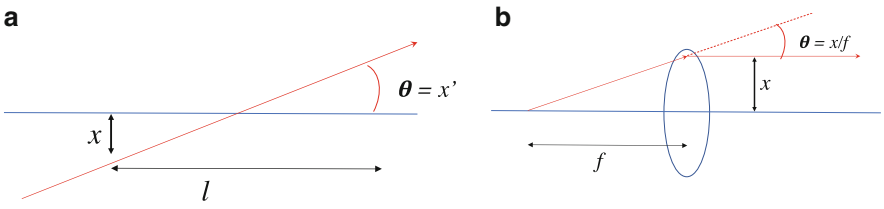

Fig. 2.8 The effect of a drift—(**a**), left side—and a focusing quadrupole lens—(**b**) right side—on a particle trajectory. The mathematical expressions are given in Eqs. (2.29) and (2.32)

A particle arriving at a quadrupole lens at a displacement x obeys Hill's equation

$$x'' + kx = 0. \tag{2.33}$$

Hence the small deflection θ is just:

$$\Delta x' = -kx\ell. \tag{2.34}$$

Comparing quadrupoles with optical lenses we remember that $\ell k = 1/f$ and is the power of the lens and that the matrix, for a thin lens, can be written:

$$\begin{pmatrix} 1 & 0 \\ -k\ell & 1 \end{pmatrix}. \tag{2.35}$$

Under the influence of these focusing and defocusing fields, a particle trajectory will finally look like a more or less zig-zag shaped curve; which for the example of eight regular cells it is shown in Fig. 2.9.

Quadrupoles are sometimes not short compared to their focal length. One must therefore use the matrices for a long quadrupole when one comes to compute the final machine:

$$\begin{aligned} M_F &= \begin{pmatrix} \cos\ell\sqrt{k} & \frac{1}{\sqrt{k}}\sin\ell\sqrt{k} \\ -\sqrt{k}\sin\ell\sqrt{k} & \cos\ell\sqrt{k} \end{pmatrix}, \text{ and} \\ M_D &= \begin{pmatrix} \cosh\ell\sqrt{k} & \frac{1}{\sqrt{k}}\sinh\ell\sqrt{k} \\ -\sqrt{k}\sinh\ell\sqrt{k} & \cosh\ell\sqrt{k} \end{pmatrix}. \end{aligned} \tag{2.36}$$

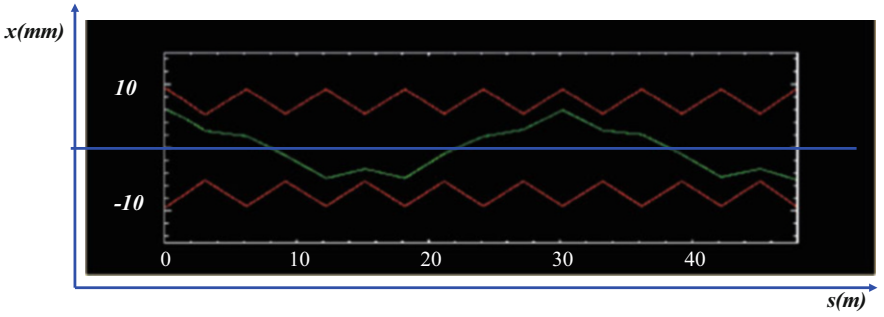

Fig. 2.9 A single particle trajectory in a ring: At each part of the lattice the amplitude and angle, (x, x′) of the particle are described by a matrix transformation, according to Eq. (2.32). The blue line corresponds to an ideal particle, with $x = x' = 0$ and so refers to the ideal orbit

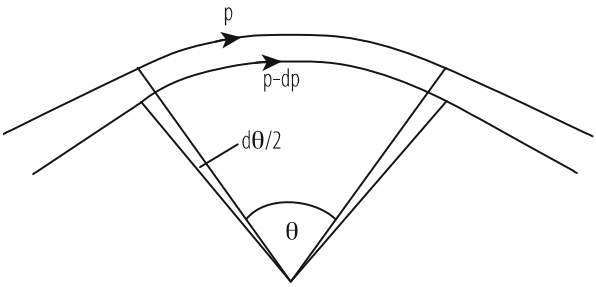

Fig. 2.10 The focusing effect of trajectory length in a pure sector dipole magnet

We can compare this with the solutions of Hill's equations within F and D quadrupoles:

$$\begin{aligned} z &= \cos\sqrt{k}\ell\ z_0 + \tfrac{1}{\sqrt{k}}\sin\sqrt{k}\ell\ z_0', \\ x &= \cosh\sqrt{k}\ell\ x_0 + \tfrac{1}{\sqrt{k}}\sinh\sqrt{k}\ell\ x_0'. \end{aligned} \tag{2.37}$$

We have so far ignored the bending that takes place in dipole magnets and these may be thought of as drift lengths in a first approximation. An exact calculation should include the focusing effect of their ends. A pure sector magnet, whose ends are normal to the beam will give more deflection to a ray which passes at a displacement x away from the centre of curvature (Fig. 2.10). This particle will have a longer trajectory in the magnet. The effect is exactly like a lens which focuses horizontally but not vertically. The matrices for a sector magnet are:

$$\begin{aligned} M_{\mathrm{H}} &= \begin{pmatrix} \cos\theta & \rho\sin\theta \\ -(1/\rho)\sin\theta & \cos\theta \end{pmatrix}, \\ M_{\mathrm{V}} &= \begin{pmatrix} 1 & \rho\theta \\ 0 & 1 \end{pmatrix}. \end{aligned} \tag{2.38}$$

Some bending magnets are not sector magnets as in Fig. 2.9, but have end faces which are parallel. It is easier to stack laminations this way than on a curve. The entry and exit angles are therefore, $\theta/2$, and the horizontal focusing effect is reduced but there is an additional focusing effect for a particle whose trajectory is displaced vertically. In the computer model one may convert a pure sector magnet into a parallel faced magnet by simply adding two thin lenses at each face. They are horizontally defocusing and vertically focusing and their strength is:

$$k\ell = -\frac{\tan\ (\theta/2)}{\rho}. \tag{2.39}$$

Unlike early lattice designers we have computers to help when we come to multiply these elements together to form the matrix for a ring or a period of the lattice [3–5]. A lattice program such as MAD [6] does all the matrix multiplication to obtain (a, b, c, d) from each specified point, s, and back again. It prints out β and φ and other lattice variables in each plane, and we can plot the result to find the beam envelope around the machine. This is the way machines are designed. Lengths, gradients, and numbers of FODO normal periods are varied to match the desired beam sizes and Q values.

In Fig. 2.8 we saw the trajectory of a particle, oscillating in a pattern of alternating focussing and defocusing quadrupoles (FODO). The trajectories in general all lie within an envelope which has the general features of the optical model in Fig. 2.6. If we were to repeat the observation of the displacement and divergence of a particle on successive turns we would find the elliptical locus of its motion (Fig. 2.5). The aspect ratio of this ellipse would depend upon where in the ring we choose to make the observation. The ellipse would be squat near D lenses and elongated near F's. The figure would appear just the same if we were to plot it between what are F quadrupoles in the vertical plane. Of course, the whole pattern of quadruples and the envelope is shifted by the distance between adjacent quadrupoles because F-quadrupoles in one plane are D in the other (et vice versa).

2.1.11 The Betatron Envelopes

To recapitulate, a modern synchrotron consists of pure bending magnets and quadrupole magnets or lenses which provide focusing. These are interspersed among the bending magnets of the ring in a pattern called the lattice. By suitable choice of strength and spacing of the lenses the envelope function $\beta(s)$ can be made periodic in such a way that it is large at all F quadrupoles and small at all D's. Symmetry will ensure this is true also in the vertical plane. Particles oscillating within this envelope will always tend to be further off axis in F quadrupoles than in D quadrupoles and there will therefore be a net focusing action. We have already seen that β is the aspect ratio of the phase space ellipse (see also [7, 8]).

In Fig. 2.11 we see an example of such a magnet pattern which is one cell, or about 1% of the circumference, of the 400 GeV SPS at CERN. Although the SPS is now considered a rather old fashioned machine its simplicity leads us to use it as an example. The focusing structure is FODO and in this pattern half of the quadrupoles (F) focus, while the other half, defocus (D) the beam. Bending magnets, which in a first approximation do no focussing are represented together with other non-focussing elements by the letter "O". The envelope of these oscillations follows a function $\beta(s)$ which has waists near each defocusing magnet and has a maximum at the centres of F quadrupoles. Since F quadrupoles in the horizontal plane are D quadrupoles vertically, and vice versa, the two functions $\beta_{\mathrm{h}}(s)$ and $\beta_{\mathrm{v}}(s)$ are one half-cell out of register in the two transverse planes. The function β has the dimensions of length but the units bear no relation at this stage to physical beam

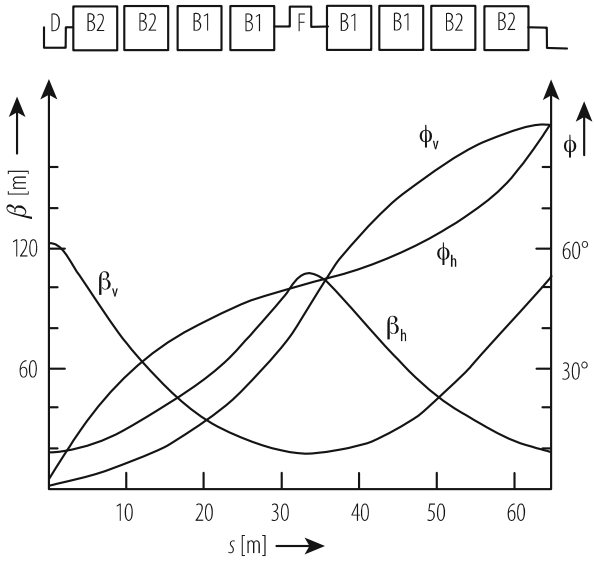

Fig. 2.11 One cell of the CERN SPS representing 1/108 of the circumference. The pattern of dipole (B) magnets and quadrupole (*F* and *D*) lenses is shown above

size. The reader should be persuaded that particles do not follow the $\beta(s)$ curves but oscillate within them in a form of modified sinusoidal motion whose phase advance is described by $\phi(s)$. The phase change per cell in the example shown is close to $\pi/2$ but the rate of phase advance is modulated throughout the cell.

2.2 Coupling

Until now we have considered the motion in the vertical and horizontal direction to be orthogonal and independent. This is the ideal case. Now we look at what happens when there is a skew quadrupole or solenoidal field in the machine which couples horizontal motion into vertical and vice versa. This is rather a special case affecting mainly electron synchrotrons and the reader may choose to skip to Sect. 2.3 and leave coupling to a second reading.

In a fully coupled machine the betatron oscillations in the two transverse directions are like two harmonic oscillators which transfer energy from one to the other with a frequency which is just the difference between their Q's. They act like coupled pendula. In this way all the horizontal "emittance" can add to the vertical emittance and the beam exceeds the available vertical aperture.

The phenomenon is particularly important in electron rings. The electron beam would damp to zero emittance were it not for quantum emission in the horizontal plane exciting betatron oscillations. There is no comparable excitation in the vertical plane and only coupling of the horizontal oscillations into the vertical plane gives

the beam any vertical dimensions. Vertical emittance, and the magnet gap needed to accept it, is directly proportional to coupling.

2.2.1 Coupling Fields

There are two principal configurations of field which excite coupling. The first we shall consider is a skew quadrupole, i.e. a quadrupole whose poles lie symmetrically in the horizontal and vertical planes (Fig. 2.12).

A particle with horizontal position x, experiences not a B_z as would be the case in a normal quadrupole and which would change its x', but a B_x which together with the paraxial velocity deflects vertically in the direction of $\boldsymbol{v} \times \boldsymbol{B}$. Of course once the particle has acquired a vertical displacement z after a number of turns it experiences a vertical field, for in a skew quadrupole the field is:

$$\begin{aligned} B_x/(B\rho) &= kx, \\ B_z/(B\rho) &= -kz. \end{aligned} \tag{2.40}$$

Thus a horizontal displacement couples into the vertical plane leading to a vertical divergence and displacement. The vertical displacement goes on to couple back into the horizontal plane modifying the horizontal displacement and divergence—and so it proceeds transferring transverse momentum back and forth from one plane to the other.

A solenoid is the other field configuration that can couple the two planes but this kind of coupling is less important in synchrotrons and we leave it to the reader to consult a more exhaustive treatment of coupling in [9].

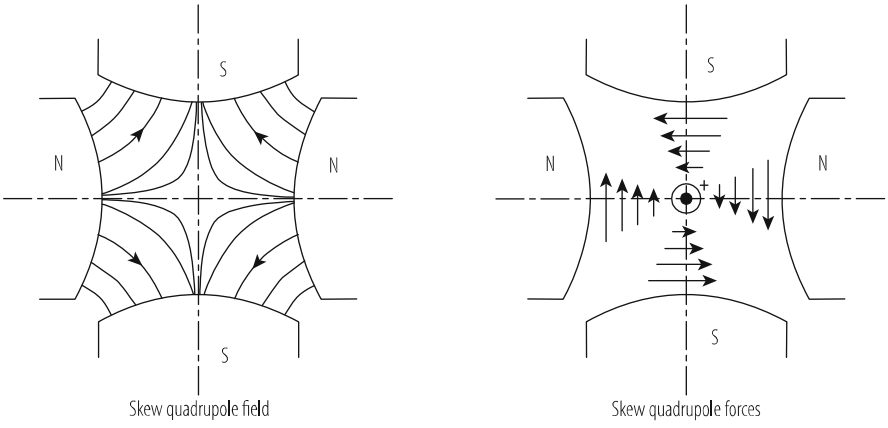

Fig. 2.12 The magnetic field and force in a skew quadrupole

2.2.2 *Qualitative Treatment of Coupling*

In our treatment the theory is deliberately simplified to reveal the physical mechanisms at work. We assume that the coupling is driven by a single skew quadrupole at the centre of one of the existing lattice machine quadrupoles where β is maximum and its derivative zero. We ignore the changes in betatron phase of one plane with respect to the other within a single turn.

The skew quadrupole gradient is normalized:

$$\begin{aligned} k &= \frac{1}{(B\rho)}\left(\frac{\partial B_x}{\partial x}\right)_{z=0}, \\ l &= \text{length of the quadrupole.} \end{aligned} \tag{2.41}$$

Figure 2.13 on the left shows the betatron motion in the horizontal plane. We have normalized the elliptical phase space trajectory into a circle at the location of the skew quadrupole by multiplying the divergence by β_x. On the right we have done the same for the vertical plane. The angular kick Δp, on passing the skew quadrupole is calculated from a similar diagram for the vertical plane and

$$\Delta p_x = \beta_x k \ell w \cos Q_{\mathrm{V}}\theta, \tag{2.42}$$

where $w = \sqrt{\varepsilon_{\mathrm{V}}\beta_z}$ is the radius of the circle for vertical motion, and $u = \sqrt{\varepsilon_{\mathrm{H}}\beta_x}$ is the radius horizontally.

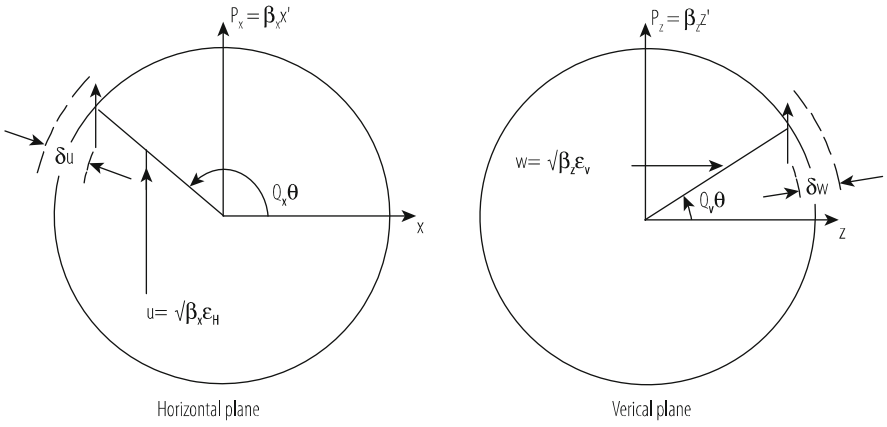

Fig. 2.13 Phase space diagram

The kick, projected as an amplitude increment becomes:

$$\delta u = w\beta_x k\ell \sin Q_{\mathrm{H}}\theta \cos Q_{\mathrm{V}}\theta. \tag{2.43}$$

When we use:

$$\sin A \cos B = \frac{1}{2}\sin(A-B) + \frac{1}{2}\sin(A+B)$$

and ignore the second, high frequency term; we obtain the coupled equations for a single passage:

$$\begin{aligned} \frac{\delta w}{w} &= -\sqrt{\frac{\varepsilon_{\mathrm{H}}}{\varepsilon_{\mathrm{V}}}}\sqrt{\frac{\beta_x\beta_z}{2}}k\ell \sin(Q_{\mathrm{H}} - Q_{\mathrm{V}})\,\theta, \\ \frac{\delta u}{u} &= \sqrt{\frac{\varepsilon_{\mathrm{V}}}{\varepsilon_{\mathrm{H}}}}\sqrt{\frac{\beta_x\beta_z}{2}}k\ell \sin(Q_{\mathrm{H}} - Q_{\mathrm{V}})\,\theta. \end{aligned} \tag{2.44}$$

These are incremental equations which we must sum over the n turns as the coupling enhances u at the expense of w.

Figure 2.14 shows diagrammatically the coupled motion. The vertical betatron amplitude decrease from $w + \Delta w$ to w in one quarter period of the slow oscillation which takes $1/4|Q_{\mathrm{H}} - Q_{\mathrm{v}}|$ turns. The mean value of the cosine is taken as $2/\pi$. We then arrive at the expressions for the maximum excursions in amplitude:

$$\begin{aligned} \frac{\Delta w}{w} &= \sqrt{\frac{\varepsilon_{\mathrm{H}}}{\varepsilon_{\mathrm{V}}}}\frac{\sqrt{\beta_x\beta_z}}{4\pi|Q_{\mathrm{H}} - Q_{\mathrm{v}}|}k\ell, \\ \frac{\Delta u}{u} &= \sqrt{\frac{\varepsilon_{\mathrm{V}}}{\varepsilon_{\mathrm{H}}}}\frac{\sqrt{\beta_x\beta_z}}{4\pi|Q_{\mathrm{H}} - Q_{\mathrm{v}}|}k\ell. \end{aligned} \tag{2.45}$$

We now move from the phase plane into real space. Some machines were designed to have a rectangular "vacuum chamber" which would accept particles which simultaneously have large horizontal and vertical "emittances". In this sense emittance is defined for a single particle

$$\varepsilon_{\mathrm{H}} = \pi u^2/\beta_x,\ \varepsilon_{\mathrm{V}} = \pi w^2/\beta_y. \tag{2.46}$$

In the presence of coupling, the particle motion is a series of Lissajous figures filling the rectangular cross-section but always touching it somewhere on each turn (Fig. 2.15). It is inevitable therefore that if coupling increases either amplitude by $\Delta u/u$ or $\Delta w/w$, some fraction of particles will be lost.

A rigorous treatment of coupling is too lengthy to include here but the reader may consult [9–11] for a complete description. This lengthier treatment leads to a model in which the modes of betatron oscillations are no longer about the vertical and horizontal planes but about two orthogonal principal planes inclined with respect to the vertical and horizontal frame.

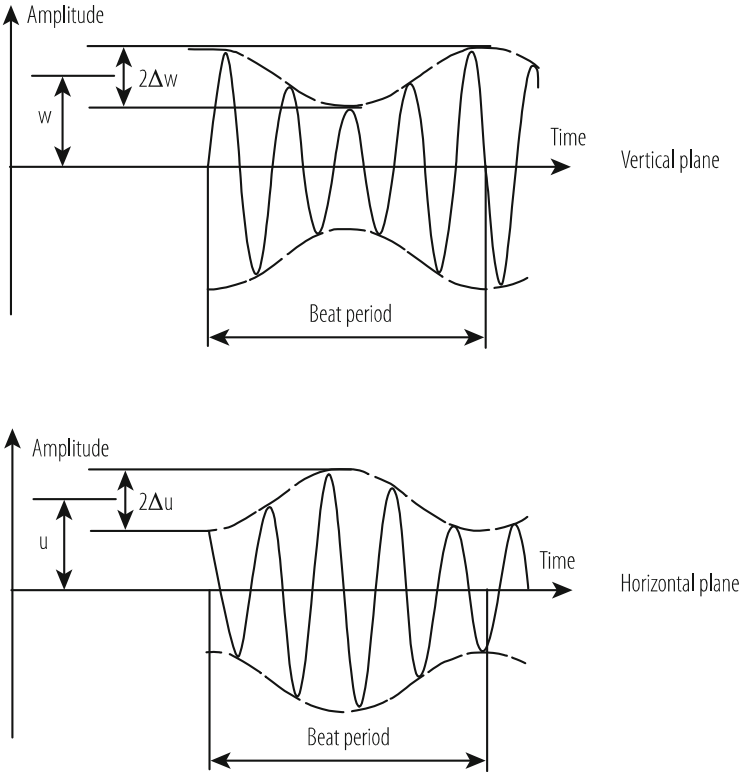

Fig. 2.14 Coupled betatron oscillations for $1/|Q_H - Q_v|$ turns

2.3 Liouville's Theorem

Now let us return to the 'mainstream' of transverse dynamics. Liouville's theorem is a conservation law that applies to the area occupied by a number of particles plotted in phase space.

We should think of a beam of particles as a cloud of points within a closed contour in a transverse phase space diagram (Fig. 2.16). Liouville's theorem tells us that this area within the contour is conserved. The contour is usually, but not always, an ellipse. In Fig. 2.5 we came across such an elliptical contour—the locus of a particle's motion plotted in phase space (x,x′) and we call its area, the emittance. We could also think of it as a limiting contour enclosing all the particles in the beam which we would again call the emittance—not of the particle but of the beam as a particle ensemble.

We express beam emittance in units of π mm·milliradians. According to Liouville the emittance area will be conserved as the beam passes down a transport line or circulates in a synchrotron whatever magnetic focusing or bending operation we do on the beam—provided that only conservative forces are taken into account.

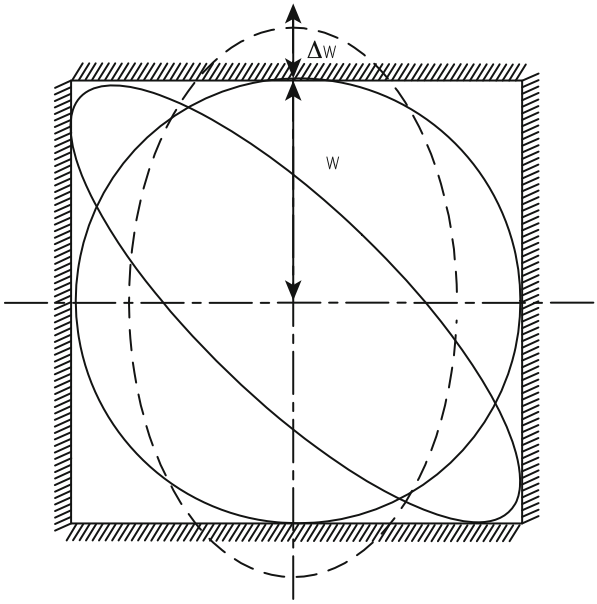

Fig. 2.15 Particle lost due to coupling

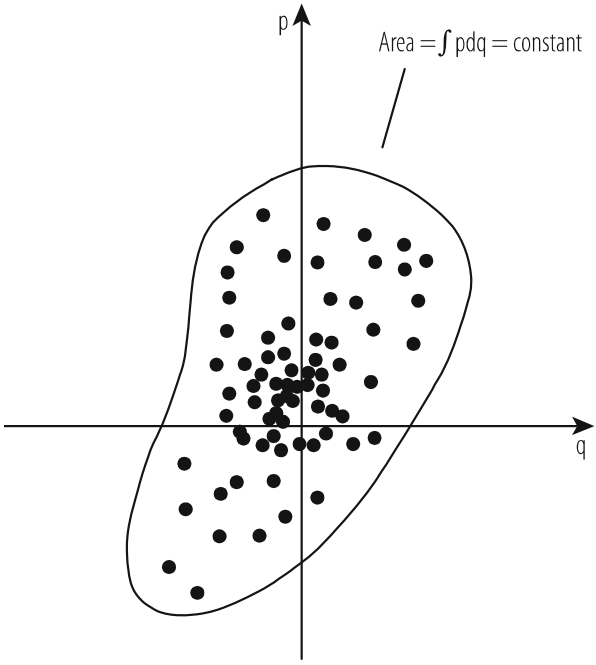

Fig. 2.16 Liouville's theorem applies to this contour

Even though the ellipse may appear to have many shapes around the accelerator its phase space area will not change (Fig. 2.17). The aspect ratio of the ellipse will change however. At a narrow waist, near a *D* quadrupole (a) in Fig. 2.17, its

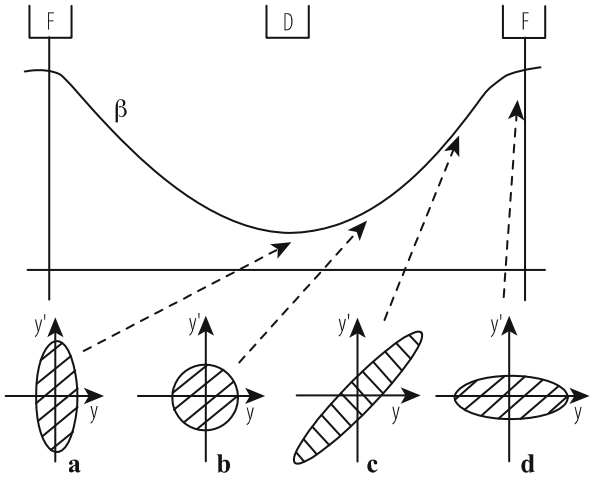

Fig. 2.17 How the conserved phase space appears at different points in a FODO cell

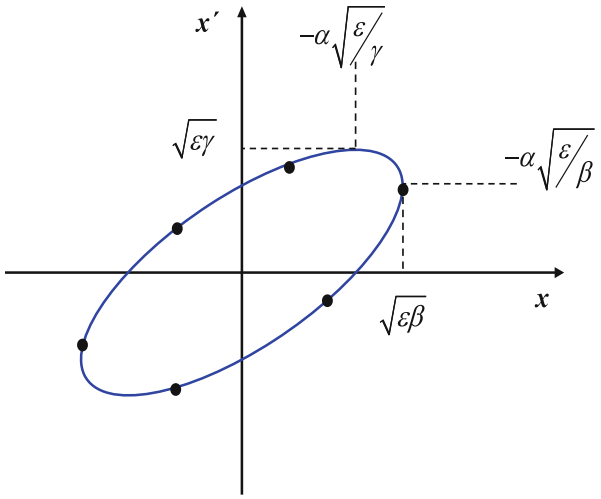

Fig. 2.18 The parameters of a phase-space ellipse containing an emittance ε at a certain point in the lattice. The shape and orientation of the ellipse are determined by the Twiss parameters at the given location

divergence will be large, while in an *F* quadrupole (d) where the betatron function is maximum, its divergence will be small. The beam is also seen at a broad waist or maximum in the beta function and a place where the beam is diverging.

In Fig. 2.18 we see how the various features of the ellipse are related to the Twiss parameters. The equation of the ellipse, often called the Courant and Snyder

invariant, has the form

$$\gamma(s)y^2 + 2\alpha(s)yy' + \beta(s)y'^2 = \varepsilon. \tag{2.47}$$

Here y is used to mean either of the transverse displacements, x or z. It is straight forward determine the relation between the shape and orientation of the (x,x′) ellipse and the Twiss parameters α, β, γ as indicated in Fig. 2.18.

The invariance of the (x,x′) space area, as we move to different points in the ring is an alternative statement of Liouville's theorem.

A word of caution—another, stricter, version of Liouville's theorem states that:

> In the vicinity of a particle, the particle density in phase space is constant if the particles move in an external magnetic field or in a general field in which the forces do not depend upon velocity.

This rules out the application of Liouville's theorem to situations in which space charge forces within the beam play a role or when there is a velocity dependent effect such as when particles emit synchrotron light. However we may apply Liouville to proton beams which do not normally emit synchrotron light and to electrons travelling for a few turns in a synchrotron. This is usually too short a time for electrons to emit enough synchrotron light energy to affect their transverse motion.

Liouville's theorem does not apply as a proton beam is accelerated. Observations tell us this is not the case. The beam appears to shrink. This is because the co-ordinates we have used so far, y and y', are not 'canonical' in the sense defined by Hamiltonian in his mechanics, which is part and parcel of Liouville's mathematical theory of dynamics. We should therefore express emittance in Hamilton's canonical phase space and relate this carefully to the co-ordinates, displacement, y, and divergence, y', which we have been using so far. We can then define an emittance which is conserved even as we accelerate.

We shall have to be particularly careful not to confuse Twiss parameters, and the parameters of special relativity: In special relativity we use β as the ratio of the particles velocity and the speed of light and the Lorentz factor γ describes the total energy divided by the rest energy. The reader will have to examine the context to be sure. For those who have not met Hamiltonian mechanics, it is sufficient to know that the canonical co-ordinates of relativistic mechanics are:

$$p = \frac{m_0\dot{y}}{\sqrt{1 - v^2/c^2}}, q = y. \tag{2.48}$$

Here q or y is a general transverse co-ordinate, p its conjugate momentum and we define β and γ when used in the context of special relativity to be:

$$\begin{aligned} &\beta = v/c, \\ &\gamma = 1/\sqrt{1 - \beta^2}, \\ &m_0 = \text{rest mass}, \\ &c = \text{velocity of light}. \end{aligned} \tag{2.49}$$

We may find the relationship between canonical momentum and divergence from the substitution:

$$p_y = m_0 \frac{dy}{dt}\gamma = m_0 \frac{ds}{dt}\frac{dy}{ds}\gamma = mc\,(\beta\gamma)\,y'. \tag{2.50}$$

Writing Liouville's Theorem expressed in canonical coordinates we can use the above expression to define a conserved quantity and relate it to the area in (y, y') space

$$\int p_y dy = m_0 c\,(\beta\gamma) \int y' dy = p_0 \int y' dy \tag{2.51}$$

where p_0 is the momentum in the direction of motion of the particle.

This invariant is the emittance, ε, of our transverse phase space multiplied by the relativistic $\beta\gamma$ which is proportional to momentum. Accelerator physicists often call this the invariant or 'normalised' emittance:

$$\varepsilon^* = \beta\gamma\varepsilon \ \ [\pi \text{ mm} \cdot \text{mrad}] \tag{2.52}$$

This normalised emittance, ε_*, is conserved as acceleration proceeds in a synchrotron and the physical emittance within the right-hand side of the equation must fall inversely with momentum if the whole term is to be conserved. Close to the velocity of light this implies that it is inversely proportional to energy.

$$Emittance = \pi\varepsilon = \int y' dy = \pi\varepsilon^* / (\beta\gamma) \propto 1/p_0. \tag{2.53}$$

We therefore expect the beam dimensions to shrink as (Fig. 2.19) a phenomenon called 'adiabatic damping'.

2.3.1 Chains of Accelerators

As a consequence of the adiabatic shrinking, the beam emittance is largest at low energy, and so is the beam dimension. Proton accelerators need their full aperture at injection and it is then that their design is most critical. For this reason it is economic to split a single large ring into a chain of accelerators—the smaller radius rings having a large aperture while the higher energy rings with large radius can have smaller apertures. In these chains of proton accelerators, such as the CERN accelerator complex, Linac – Booster – PS – SPS, the invariant emittance, determined by the parameters of the beam as it leaves the ion source at the beginning of the linac, may be conserved to several hundred GeV. Of course one must guard against mismatches between machines or non-linear fields which dilate the emittance.

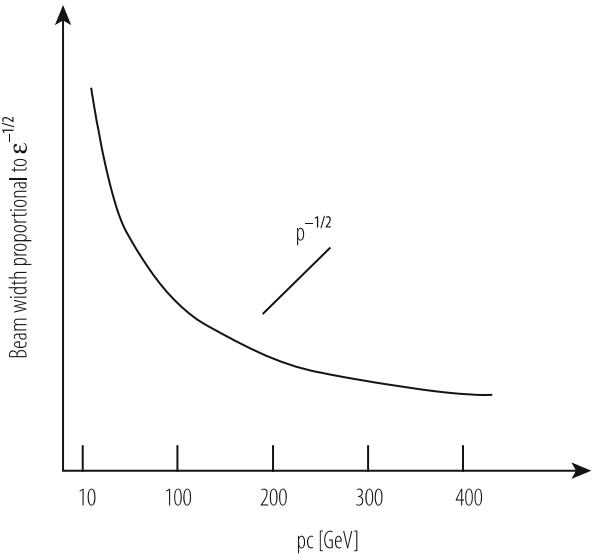

Fig. 2.19 Adiabatic shrinking of the beam as function of the beam momentum during acceleration

2.3.2 Exceptions to Liouville's Theorem

The invariance of normalised emittance of a proton beam and the shrinking of its physical emittance with energy is quite the opposite of what happens in an electron machine. Liouville's theorem only applies to conservative systems, where particles are guided by external fields and not to electron machines where particles emit some of their own energy. Electrons, being lighter than protons and hence more relativistic, emit quanta of radiation as they are accelerated. This quantised emission causes particles to jump around in momentum, leading to changes in the trajectories amplitude and angle. These changes couple into both planes of transverse phase space. At the same time, there is a steady tendency for particles near the edge of the emittance to lose transverse energy and fall back towards the centre. In an electron machine the emittance is determined not by the Liouville but by the equilibrium between these two effects. In fact, it grows with E^2.

Consider a number of protons which have the maximum amplitude present in the beam. They follow trajectories at the perimeter of the ellipse but at any instant have a random distribution of initial phases ϕ_0. If we were able to measure y and y' for each and plot them in phase space, they would lie around the ellipse of area $\pi\varepsilon$ and their co-ordinates would lie in the range of

$$\begin{aligned} -\sqrt{\beta\varepsilon} \le y \le \sqrt{\beta\varepsilon}, \\ -\sqrt{\varepsilon\gamma} \le y' \le \sqrt{\varepsilon\gamma}. \end{aligned} \tag{2.54}$$

Particles in a beam are usually distributed in a population which appears Gaussian when projected on a vertical or horizontal plane. In a proton machine

the emittance boundary used to be conventionally chosen to be that of a proton with amplitude 2σ. This would include about 90% (strictly 87%) of a Gaussian beam where σ is the standard distribution. In an electron machine a 2σ boundary would be too close to the beam and an aperture stop placed at this distance would rather rapidly absorb most of the beam as particles redistribute themselves, moving temporarily into the tails due to quantum emission and damping. The safe physical boundary for electrons depends on the lifetime required but is in the region of 6σ to 10σ. The emittance which is normally quoted for an electron beam corresponds to an electron with the amplitude of σ in the Gaussian projection. We are then free to choose how many σ's we must allow. There is consequently a factor 4 between emittance defined by electron and proton experts.

2.4 Momentum Dependent Transverse Motion

In the previous chapters, we have studied the motion of a particle as it swings from side to side about the ideal orbit around the synchrotron: the transverse motion. Nothing is perfect, however, and so we cannot assume that each and every proton in a large ensemble of up to 10^{11} particles will have exactly the ideal momentum. Instead we expect a certain momentum spread in the beam and therefore we have to study how transverse motion depends on small departures, $\Delta p/p_0$, from the synchronous momentum p_0.

2.4.1 Dispersion

The central closed orbit of a synchrotron is matched to an ideal (synchronous) momentum p_0. A particle of this momentum and of zero betatron amplitude will pass down the centre of each quadrupole, be bent by exactly 2π by the bending magnets in one turn of the ring and remain synchronous with the r.f. frequency. Its path is called the central (or synchronous) momentum closed orbit. In Fig. 2.8 this ideal orbit is the horizontal axis and we see particles executing betatron oscillations about it but these oscillations do not replicate every turn. The synchronous orbit, however, closes on itself so that x and x' remain zero.

We now consider a closed orbit which is distorted in the horizontal plane by non-ideal bends in the dipole. Figure 2.20 shows a particle with a lower momentum $\Delta p/p < 0$ and which is bent horizontally more in each dipole of a FODO lattice. We could argue that the total deflection, being more than 2π would cause it to spiral inwards and hit the vacuum chamber wall. On the other hand there is a closed orbit for this lower momentum in which the extra bending forces are compensated by extra focusing forces as the orbit is displaced inwards in the F quadrupoles and less so in the defocusing in the D's (Fig. 2.20). We may describe the shape of this new closed orbit for a particle of unit $\Delta p/p$ by a *dispersion* function $D(s)$. The

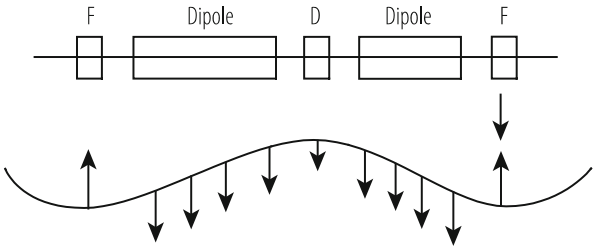

Fig. 2.20 The extra inward force given to a low momentum particle by the dipoles is balanced by the focusing the quadrupoles and defines a dispersion function

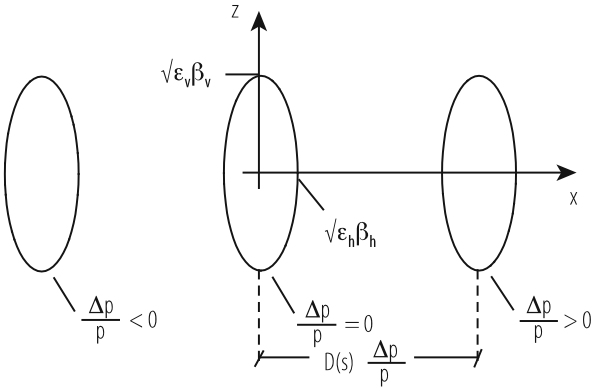

Fig. 2.21 The beam cross sections in real space for beams of three different momenta at a point where the dispersion function is large

displacement of the closed orbit is:

$$x(s) = D(s)\frac{\Delta p}{p_0}. \tag{2.55}$$

In Fig. 2.21 we see how the effect of dispersion for off momentum orbits adds to the betatron motion to widen the beam cross section. The betatron motion of each of the three particles: $\Delta p/p < 0$, $\Delta p/p = 0$, and $\Delta p/p > 0$, is within an ellipse in physical (x, z) space. The ellipses for each momentum are separated by a distance $D(s)\Delta p/p$. The semi-aperture required will be:

$$a_{\mathrm{V}} = \sqrt{\beta_{\mathrm{V}}\varepsilon_{\mathrm{V}}}, a_{\mathrm{H}} = \sqrt{\beta_{\mathrm{H}}\varepsilon_{\mathrm{H}}} + D(s)\frac{\Delta p}{p}. \tag{2.56}$$

2.4.2 Chromaticity

This effect is equivalent to the chromatic aberration in a lens. It is defined as a quantity Q':

$$\Delta Q = Q'\frac{\Delta p}{p}. \tag{2.57}$$

The chromaticity [12] arises because the focusing strength of a quadrupole has $(B\rho)$ in the denominator and is therefore inversely proportional to momentum:

$$k = \frac{1}{(B\rho)} \frac{dB_z}{dx}. \tag{2.58}$$

A small spread in momentum in the beam, $\pm\, \Delta p/p$, causes a spread in focusing strength:

$$\frac{\Delta k}{k} = \mp \frac{\Delta p}{p}. \tag{2.59}$$

Integrated over all focusing (and defocusing) elements in the ring, we obtain a change in the tune of the machine

$$\Delta Q = \frac{1}{4\pi} \int \beta(s)\delta k(s) ds. \tag{2.60}$$

This enables us to calculate Q':

$$\Delta Q = \frac{1}{4\pi} \int \beta(s)\delta k(s) ds = \left[\frac{-1}{4\pi} \int \beta(s) k(s) ds \right] \frac{\Delta p}{p}. \tag{2.61}$$

The quantity in square brackets is the chromaticity Q'. To be clear, this is called the natural chromaticity. For most alternating gradient machines, its value is about $-1.3Q$. Of course there are two Q values relating to horizontal and vertical oscillations and therefore two chromaticities. Chromaticity may be corrected with sextupole magnets (see Chap. 3, and Sects. 6.1 and 8.1).

2.5 Longitudinal Motion

2.5.1 Stability of the Lagging Particle

Suppose two particles are well below the velocity of light. A particle *A,* that arrives at the right moment to in the RF resonator and thus will obtain exactly the right acceleration voltage. We call this particle "*synchronous*" (see Fig. 2.22). A second particle, *B*, arrives late, and so receives an extra energy increment which will cause it to speed up and overtake the synchronous particle, *A*. In so doing, its energy defect, ΔE, grows and, provided the amplitude is not too large, its trajectory will follow an ellipse in phase space. This describes this motion up and down the r.f. wave (Fig. 2.22) and may remind some readers of the representation of a simple harmonic oscillator, or pendulum. When plotted in a phase space diagram of velocity versus longitudinal displacement we indeed obtain a shape that is elliptical. The trajectory

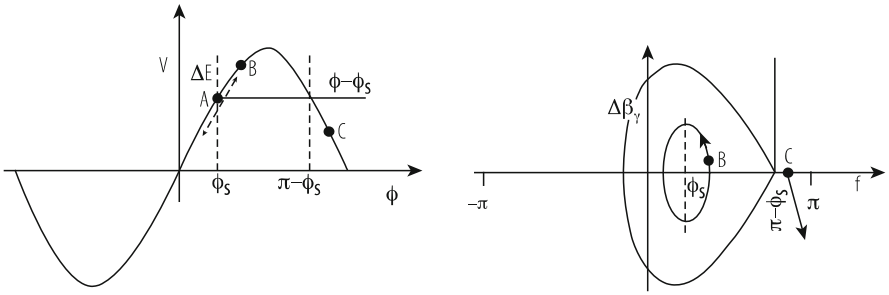

Fig. 2.22 The limiting trajectory for a particle in a 'moving' or accelerating bucket when the stable phase is not zero

of this longitudinal movement in phase space is closed and over many turns the average deviation from the synchronous energy is zero. This *phase stability* depends upon the fact that δE is positive when $\phi - \phi_s$ is small and positive [13, 14].

When a particle reaches the non-linear part of the r.f. wave and over the top of the wave, it will still be restored and oscillate about the stable phase provided it does not reach and pass the point where it receives less incremental energy than the synchronous particle. On this non-linear part of the curve the motion is no longer an ellipse but is distorted into a fish-shape but its trajectory is still closed and stable. However, if a particle, C, oscillates with such large amplitude that it falls below the synchronous voltage, an increase in ϕ will cause a negative ΔE which in turn causes ϕ to move further away from the synchrotron particle. This particle is clearly unstable and will be continuously decelerated. There is a particle which, starting at $\phi = \pi - \phi_s$, would trace out a limiting fish-shaped trajectory which is the boundary or *separatrix* between stable and unstable motion. The region within this separatrix is called the r.f. bucket and is shown in the lower half of Fig. 2.22. Formulae for the calculation of the parameters of moving buckets are to be found in [15].

Let us look more carefully at the argument that a particle, arriving late because of its lower energy, would see a higher RF voltage from the rising waveform and, accelerated to a higher velocity, would catch up with the synchronous particle. Dispersion may make the situation more complicated. Giving the errant particle more energy will speed it up but may also send it on an orbit of larger radius.

The path length that the particle, B, must travel around the machine, or more correctly, the change in path length with momentum, must depend upon the dispersion function. The closed orbit will have a mean radius:

$$R = R_0 + \overline{D}\frac{\Delta p}{p}. \tag{2.62}$$

Close to the velocity of light where acceleration can increase momentum but not velocity, the longer path length will more than cancel the small effect of velocity and the particle, instead of catching up with its synchronous partner, will arrive

even later than it did on the previous turn. This seems to defeat the whole idea of phase stability. Depending on how the synchrotron is designed and which particles it accelerates, there can be a certain energy where our initial ideas of phase stability break down. This is called the transition energy. Fortunately there is also a way of ensuring stability above transition.

2.5.2 Transition Energy

The rigorous argument to resolve the question of velocity versus path length is to examine how the revolution time (or its reciprocal, the revolution frequency) varies as the particle is given extra acceleration. The revolution frequency is:

$$f = \frac{\beta c}{2\pi R}, (\beta = v/c)\,. \tag{2.63}$$

This revolution frequency, f, depends on two momentum dependent variables, the relativistic β=v/c and R, the mean radius. The penultimate equation gives the change in the radius. The momentum dependence of β is determined by:

$$p = \frac{E_0\beta}{\sqrt{1-\beta^2}}. \tag{2.64}$$

The rate of "catching up" depends upon a "slip factor", η, which is defined as logarithmic differential of frequency as a function of momentum. The procedure of partial derivatives tells us there must be two terms. Hence:

$$\eta_{\mathrm{rf}} = \frac{\Delta f/f}{\Delta p/p} = \frac{p}{\beta}\frac{d\beta}{dp} - \frac{p}{R}\frac{dR}{dp} = \frac{1}{\gamma^2} - \frac{\overline{D}}{R_0}. \tag{2.65}$$

The first term on the right-hand side describes the increase in speed with p and the other (negative), how the path to be completed increases with p.

The second term is energy independent while the first term shrinks as acceleration proceeds. At low energy this is largest and η is >0. But, since $\gamma = E/E_0$, the first term becomes smaller than the second at high energy so that η changes sign from positive to negative. During the acceleration process there is a certain energy, the transition energy, at which η is momentarily zero. At transition, the value of γ satisfies:

$$\frac{1}{\gamma_{\mathrm{tr}}^2} = \frac{\overline{D}}{R}. \tag{2.66}$$

In proton synchrotron design this condition tends to be encountered mid–way through the acceleration cycle and can only be avoided with some ingenuity in the design of the lattice. This was a worry to the designers of the PS and AGS, the

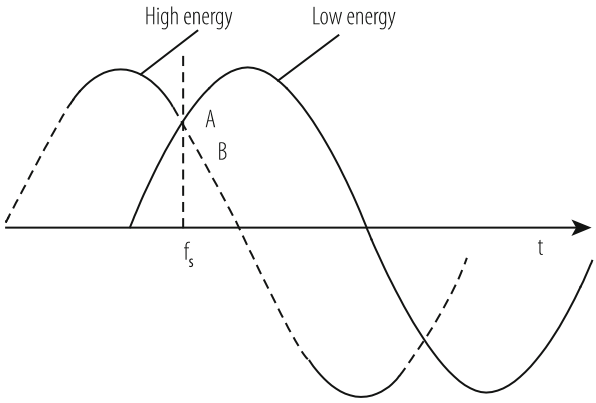

Fig. 2.23 Shows how changing the phase of the RF voltage waveform can give the lagging particle, B, less energy rather than more and lead to stability above transition

first proton synchrotrons of high enough energy to encounter this problem during acceleration but it was then realised that one could, almost instantaneously, change the phase of the voltage wave in the RF cavities to be falling rather than rising at the moment of the synchronous particles arrival (see Fig. 2.23). With such a reversed slope, particles arriving late are given less than their ration of energy and take a inner circular path—a short cut—to arrive earlier next time.

Electron machines are fortunate in that due to the small rest mass their Lorentz factor γ, being 2000 times higher, ensures that the first term may be neglected and such machines operate always above transition.

2.5.3 Synchrotron Motion

If we consider the motion of a particle on the linear part of the voltage wave of an r.f. cavity it is not difficult to imagine that it approximates rather closely to a harmonic oscillator. Unlike to the situation in the transverse plane, however, the motion becomes more complicated when the oscillation amplitude is larger, and the particle feels the non-linear part of the sinusoidal RF wave, or even more, for part of its motion it finds itself over the crest of the wave. But first let us focus on a small amplitude solution.

It is not hard to deduce from special relativity that the momentum may be written

$$p = m_0 c\,(\beta\gamma)\,. \tag{2.67}$$

The quantity $\Delta(\beta\gamma)$ serves as the momentum co-ordinate in longitudinal phase space. The other co-ordinate is the particle's arrival phase, ϕ, with respect to the zero crossing of the r.f. voltage at the cavity. Let us consider the simplest case of a small oscillation in a stationary bucket, $\phi_s = 0$ (when the particle is not being accelerated).

A particle with a small phase error will describe an ellipse in phase space which one may write parametrically as

$$\begin{aligned} \Delta(\beta\gamma) &= \widehat{\Delta(\beta\gamma)}\sin 2\pi f_s t, \\ \phi &= \hat{\phi}\cos 2\pi f_s t, \end{aligned} \tag{2.68}$$

where f_s is the frequency of execution of these oscillations in phase which we call the synchrotron frequency.

To reveal the differential equation behind this motion we must first remember that the angular frequency $2\pi f$ of an oscillator is nothing other than the rate of change of phase, $\dot{\phi}$ or to be exact $-\dot{\phi}$. (The negative sign stems from the fact that ϕ is a phase lag.) We may therefore relate the rate of change in arrival phase to the difference in revolution frequency of the particle, compared to that of the synchronous particle.

$$\dot{\phi} = -2\pi h\left[f(\Delta\beta\gamma) - f(0)\right] = -2\pi h\Delta f. \tag{2.69}$$

We have multiplied by, h, the harmonic number of the r.f. since ϕ is the phase angle of the r.f. swing while $f(\Delta\beta\gamma)$ is the revolution frequency. Here we can use the definition of the slip factor η and then simply use some standard relativistic relations to end up with Δf as a function of ΔE, the energy defect with respect to the synchronous particle:

$$\Delta f = \eta f\frac{\Delta p}{p} = \eta f\frac{\Delta(\beta\gamma)}{(\beta\gamma)} = \frac{\eta f}{\beta^2}\frac{\Delta\gamma}{\gamma} = \frac{\eta f}{E_0\beta^2\gamma}\Delta E. \tag{2.70}$$

where E_0 the total energy (including its rest mass) of the synchronous particle.

We differentiate once more to obtain a second order differential equation which we hope to resemble a simple oscillator.

$$\ddot{\phi} = -\frac{2\pi h\eta f}{E_0\beta^2\gamma}\left(\Delta\dot{E}\right). \tag{2.71}$$

The extra energy given per turn to a particle whose arrival phase is ϕ will be

$$\Delta E = eV_0\left(\sin\phi - \sin\phi_s\right), \tag{2.72}$$

and the rate of change of energy will be this times, f, the revolution frequency. So we can write

$$\ddot{\phi} = -\frac{2\pi eV_0 h\eta f^2}{E_0\beta^2\gamma}\left(\sin\phi - \sin\phi_s\right). \tag{2.73}$$

This is a fundamental and exact description of the motion provided the parameters should change slowly (the adiabatic assumption). We can simply integrate to

find its solution numerically but to see an analytic solution for small amplitudes we set $\phi_s = 0$ and $\phi \approx \sin\phi$:

$$\ddot{\phi} + \frac{2\pi e V_0 h \eta f^2}{E_0 \beta^2 \gamma} \phi = 0. \tag{2.74}$$

The frequency of these synchrotron oscillations in longitudinal phase space is

$$f_s = \sqrt{\frac{|\eta|\, he V_0}{2\pi\, E_0 \beta^2 \gamma}}\, f, \tag{2.75}$$

or writing $f_{rf} = hf$ we could equally express

$$f_s = \sqrt{\frac{|\eta|\, e V_0}{2\pi\, E_0 \beta^2 \gamma h}}\, f_{rf}. \tag{2.76}$$

In analogy to the transverse plane, we define a synchrotron tune, Q_s, as the number of such oscillations per revolution of the machine. This is analogous to Q in transverse phase space.

$$Q_s = \frac{f_s}{f} = \sqrt{\frac{|\eta|\, eh V_0 \cos\phi_s}{2\pi\, E_0 \beta^2 \gamma}}. \tag{2.77}$$

Usually Q_s is less than 10% of the revolution frequency. It drops down to zero at γ transition where η is zero and then rises again. In large proton machines it can be in the region 0 to 100 Hz and, but for the vacuum, one might hear it!

Close to γ_{tr} we cannot strictly assume that β, γ, η, and f vary slowly in comparison with the synchrotron oscillation which this equation describes. Hence we should use a more exact form of the equation of motion and approximate only when it seems that this is justified:

$$\frac{d}{dt}\left[\frac{E_0 \beta^2 \gamma \dot{\phi}}{2\pi \eta h f^2}\right] + e V_0 (\sin\phi - \sin\phi_s) = 0. \tag{2.78}$$

In a stationary bucket, when $\phi_s = 0$, this exact differential equation for large amplitude motion is identical to that for a rigid pendulum:

$$\ell \frac{d^2\theta}{dt^2} + g \sin\theta = 0. \tag{2.79}$$

There is an extra term, $\sin\phi_s$, on the right hand side of the synchrotron equation which is not there in the pendulum case but it could be introduced too for the pendulum by using a magnetic 'bob' and biasing its equilibrium position to one side by attaching a weight on a cantilever at right angles to the rod of the pendulum.

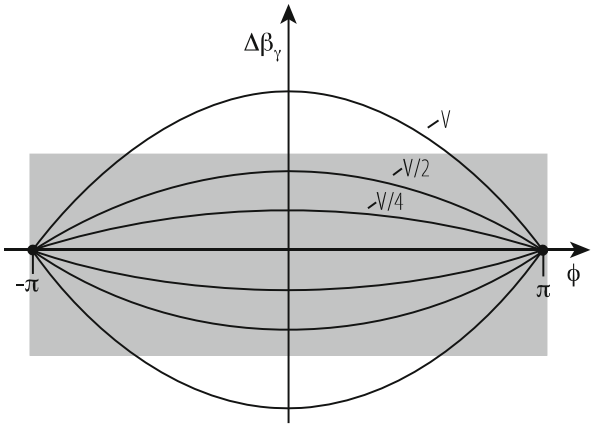

Fig. 2.24 Adiabatic trapping of coasting beam in growing stationary bucket

In fact the unbiased pendulum corresponds to synchrotron motion when there is no acceleration—we say the bucket is stationary. In Fig. 2.22 we saw how particles close to the edge of the stable area of the bucket follow a fish-shaped trajectory when $\phi_s = 0$; before acceleration starts or when the beam is held at the same energy in collider mode (see Fig. 2.24).

In order to accelerate ϕ_s must be made finite, in which case the figure changes somewhat. The stable area becomes smaller and shaped like a fish—or rather a series of fish chasing each other's tails. Small amplitude motion will still be sinusoidal but the ellipse will be centred on the stable phase ϕ_s and not on $\phi = 0$.

2.5.4 Stationary Buckets

The size of the bucket depends on how close the stable phase, ϕ_s is to the crest of the sine-wave. It shrinks to zero if $\phi_s = 90°$. There is a special case if ϕ_s is zero. This is often the case as a beam injected into a synchrotron before acceleration has started or in a collider where the r.f. simply holds the bunches together. The bucket is then said to be 'stationary' stretching over all phases from $-\pi$ to π. Its height is the range of energies $2\Delta E$ which the r.f. wave can constrain and this turns out to be dependent on $\sqrt{V}$ for a given ϕ_s. If V is reduced, the more energetic particles spill out of the bucket.

Very often the particles are injected as a continuous ribbon without any longitudinal structure crosshatched in Fig. 2.24. Usually acceleration has not yet started, the magnetic field B is constant, and ϕ_s is zero. If V is increased slowly, the height of the stationary bucket grows, and more and more of the energy spread in the beam, ΔE, is trapped (Fig. 2.24). This is called "adiabatic trapping".

References

1. E.D. Courant, H.S. Snyder: Annals of Physics 3 (1958) 1–48.
2. J.J. Livingood: *Principles of cyclic particle accelerators*, van Nostrand (1961).
3. R. Servranckx, K.L. Brown: SLAC Report 270 UC-288 (1984).
4. A.A. Garren, A.S. Kenney, E.D. Courant, M.J. Syphers: Fermilab report FN40 (1985).
5. L. Schachinger, R. Talman: SSC Report-52 (1985).
6. F.C. Iselin, H.G. Grote: CERN/SL/90-13 (1991).
7. P. Schmüser: CERN 87-10 (1987).
8. J. Rossbach, P. Schmüser: CERN 94-1 (1992).
9. P. Bryant: CERN ISR-MA/75-28 (1975).
10. J.P. Koutchouk: CERN ISR-OP/80-27 (1980).
11. G. Guignard: CERN 76-06 (1976).
12. S. Guiducci: CERN 94-01 (1992).
13. B.W. Montague: CERN 77-13 (1977).
14. J. Le Duff: CERN 94-01 (1992).
15. C. Bovet, R. Gouiran, I. Gumowski, H. Reich: CERN/MPS-SI/Int.DL/70/4 (1970).